Desalination and Water Treatment
www.deswater.com
doi: 10.1080/19443994.2015.1043951

57 (2016) 11184–11194
May

Taylor & Francis
Taylor & Francis Group

Experimental and modeling of nickel removal from sulfate solutions by emulsion liquid membrane using PC 88A

Lelin Zeng[a], Weiyan Wang[a], Wei Chen[a], Caroline Bukirwa[a,b], Yunquan Yang[a,*]

[a] *School of Chemical Engineering, Xiangtan University, Xiangtan City, Hunan 411105, P.R. China, Tel. +86 731 58298809; Fax: +86 731 58293801; emails: zenglelin2013@126.com (L. Zeng), wangweiyan@xtu.edu.cn (W. Wang), chenweixtu@163.com (W. Chen), bukcaro2009@yahoo.com (C. Bukirwa), yangyunquan@xtu.edu.cn (Y. Yang)*
[b] *School of Public Health, Makerere University, P.O. Box 7072, Kampala, Uganda*

Received 24 September 2014; Accepted 1 April 2015

ABSTRACT

The removal of nickel from sulfate media using emulsion liquid membrane with PC 88A as carrier was studied by simulation and experimental method. Combining reasonable assumptions from the existing models, a modified mathematical model was developed. It was assumed that the concentrations at the external interface were in dynamic equilibrium. The mass transfer rate of the nickel–carrier complexes at the interface of the emulsion droplet and that of the nickel ions in the external feed solution were assumed to be equal. According to these modifications, the computational results could agree well with the experimental data. The total average value of the squared residuals was less than 0.022. The effects of agitation speed, volume ratio, and the concentration of the nickel ions and that of the PC 88A on the removal rate of nickel were investigated. The concentration of the PC 88A has shown greater influence on the nickel removal in comparison with the other parameters. Under typical conditions, the removal of nickel reached 93% in 10 min. According to the simulated results of the model, the concentration variations at the external interface and in the emulsion globule were showed and discussed, respectively.

Keywords: Emulsion liquid membrane; Nickel removal; PC 88A; Model

---

1. Introduction

Nickel and its compounds are widely used in many industrial processes such as electroplating, metallurgy, and machine manufacturing. As a result, a large amount of nickel wastewater is produced during industrial processes. Nickel is known as toxic metal which can be bioaccumulated through the food chain, and can negatively affect the organisms. On the other hand, the spent liquor containing nickel is a recyclable and valuable resource. In the traditional solvent extraction process for cobalt and nickel separation, cobalt ions can be preferentially extracted by the organophosphorus reagents. Few studies were carried out in the field of concentration and extraction of nickel from the cobalt raffinate by the solvent extraction [1]. However, the extraction ability of nickel with the organophosphorus reagents was always poor, especially under the low pH values conditions. The emulsion liquid membrane (ELM) technique is considered to be a potential separation and enrichment technology for the removal of nickel, because of its rapid

---

*Corresponding author.

rate of mass transfer, good selectivity, and high efficiency. Since the development of the ELM, this technique has been broadly used in the studies for the purification of metal ions [2,3], organics [4–6], and the removal of heavy metal ions [7].

Some researches have been reported on the treatment of nickel wastewater by the ELM. Kumbasar and Kasap [8,9] investigated the carriers of 8-hydroxyquinoline and 5,7-dibromo-8-hydroxyquinoline for the nickel extraction. The drop size distribution and the mean diameter of the emulsion drops were studied by Chakraborty et al. [10]. The effects of various stripping acids and different operating conditions on the stability of the ELM system and the recovery of nickel were explored in studies by Kulkarni et al. [11,12]. The above studies were mainly aimed at obtaining the optimal technological conditions for the extraction of nickel by the ELM process. However, it is indispensable to thoroughly investigate the mass transfer mechanism of the ELM.

A number of studies have been carried out on the mathematical descriptions for the mass transfer mechanism of the ELM. Kopp et al. [13] considered the unsteady-state diffusion in the emulsion globules into their model. Ho et al. [14] improved this model into a well-known advancing front model. Chakraborty et al. [10] considered the effect of the emulsion globules with different diameters into the advancing front model. Yan et al. [15] developed a simultaneous diffusion- and reaction-controlled model. The assumption of reaction irreversibility is the shortcoming of the advancing front model. The advancing front models and the reversible reaction model were compared to describe 2-chlorophenol extraction by the ELM [16]. Reis et al. [17–19] further developed the reversible reaction model in their works.

The organophosphorus extractants of D2EHPA (di (2-ethylhexyl)phosphoric acid), PC 88A (2-ethylhexyl phosphonic acid mono-2-ethylhexyl ester), and Cyanex272 (bis(2,4,4-trimethylpentyl)phosphinic acid) were extensively studied in solvent extraction and even in the ELM. Comparing the three above carriers, D2EHPA has been investigated deeply in several studies for nickel extraction. Cyanex272 is a potential carrier, particularly in the separation process. Nonetheless, Cyanex272 is expensive and the pH value of the external aqueous phase in the system of Cyanex272 should be high to obtain better extraction rate of nickel. There are very few researches on the nickel extraction by the ELM using PC 88A. Hence, PC 88A was chosen as carrier in this work for the removal of nickel ions from sulfate media by the ELM. In the aspect of modeling, to overcome the shortcomings of the mentioned above models, we combined the reasonable assumptions from the two models presented by Reis et al. [18] and Lee et al. [20] and developed a modified model to analyze the mass transfer mechanism of the nickel removal by the ELM using PC 88A.

2. Mathematical modeling

As mentioned above, the two models proposed by Reis et al. [18] and Lee et al. [20] did not elaborate how to describe the concentration variation of the substances at the interface of III/II. In this paper, a modified model was proposed in which it was assumed that a dynamic equilibrium could be reached between the concentration of the nickel ions and the carrier when they contacted at the interface of III/II. Furthermore, the mass transfer rate of the nickel ions in the external aqueous phase and the nickel–carrier complex at the interface of the emulsion droplet were equal. These assumptions were described by three ordinary differential equations which were derived from the extraction equilibrium equation and the two other mass transfer equations as shown below (Eq. (8) and Eqs. (19)–(20)). Meanwhile, the initial concentration values of the substances at the external interface were assumed to be in equilibrium, because the reaction rate is very rapid at the beginning of the extraction reaction. Thus, the values of the initial concentration could be calculated according to the Eqs. (7) and (18). All of the modifications above resulted in the present model as shown below.

The mass transfer in the feed solution and the emulsion droplets, the extraction and stripping reactions at the interfaces were studied, as shown in Fig. 1. Except for the mass transfer in the crust of the emulsion droplet, which was taken into account, the model assumptions were same as the mentioned above model [18]. Moreover, at the interface of III/II, the reaction time to reach the equilibrium at the beginning of the extraction reaction is considered to be near 0.

The hydrogen ions concentration values were assumed not to vary because of the HAc–NaAc buffer solution in the external feed solution and the excess sulfuric acid in the internal stripping solution. The nickel ions are extracted by PC 88A:

$$\mathrm{Ni}^{2+} + 3\overline{(\mathrm{HR})_2} \leftrightarrow \overline{\mathrm{NiR}_2 \cdot 2(\mathrm{HR})_2} + 2\mathrm{H}^+ \qquad (1)$$

The Eq. (1) is simplified as:

$$\mathrm{Ni}^{2+} + 3\mathrm{B} \leftrightarrow \mathrm{C} + 2\mathrm{H}^+ \qquad (2)$$

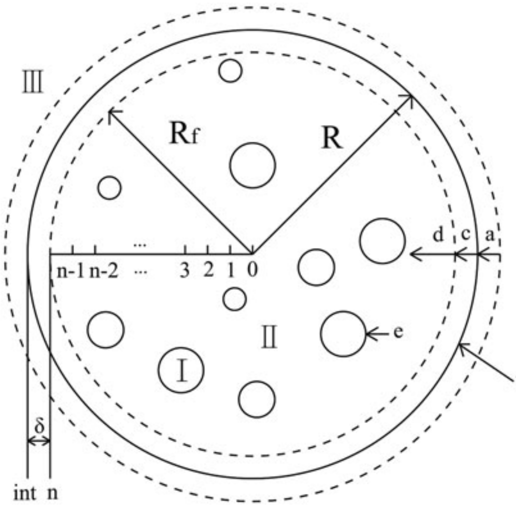

Fig. 1. Model of nickel extraction by the ELM: (a) mass transfer of nickel ions; (b) nickel ions extraction reaction; (c) diffusion in the crust of the emulsion droplet (oil layer); (d) diffusion in the water-in-oil emulsion droplet; and (e) nickel ions stripping reaction.

$$K_{\mathrm{eq}} = \frac{c_{\overline{\mathrm{NiR_2 \cdot 2(HR)_2}}} \cdot c_{\mathrm{H^+}}{}^{2}}{c_{\mathrm{Ni^{2+}}} \cdot c_{\overline{\mathrm{(HR)_2}}}{}^{3}} \, \mathrm{or} \, \frac{c_C c_{\mathrm{H^+}}{}^{2}}{c_{\mathrm{Ni^{2+}}} c_B^3} \tag{3}$$

where K_{eq} is the reaction equilibrium constant, and the extractant (HR) of PC 88A is assumed as a dimer. The concentration values of the substances at the interface of III/II are in the dynamic equilibrium. The stripping reaction of nickel is expressed as:

$$r_{\mathrm{s}} = k_{\mathrm{s}} \cdot c_{\mathrm{C}} - K_{\mathrm{eq}} \frac{c_{\mathrm{Ni^{2+}}} c_B{}^{3}}{c_{\mathrm{H^+}}{}^{2}} \tag{4}$$

The initial concentration values of hydrogen ions in the external aqueous phase and the sulfuric acid solution are estimated by the speciation of the sulfuric acid [17].

The mass transfer of $\mathrm{Ni^{2+}}$ ions:

$$-V_{\mathrm{III}} \frac{\mathrm{d}c_{\mathrm{Ni^{2+}(III)}}}{\mathrm{d}t} = S \cdot k_{\mathrm{Ni}} \left(c_{\mathrm{Ni^{2+}(III)}} - c_{\mathrm{Ni^{2+}(III),int}} \right) \tag{5}$$

where the external surface (S) is calculated by

$$S = \frac{6}{d_{32}} (V_{\mathrm{I}} + V_{\mathrm{II}}) \tag{6}$$

The dynamic reaction equilibrium equation at the interface of III/II:

$$K_{\mathrm{eq}} = \frac{c_{\mathrm{C(II),int}} \cdot c_{\mathrm{H^+(III),int}}{}^{2}}{c_{\mathrm{Ni^{2+}(III),int}} \cdot c_{B\mathrm{(II),int}}{}^{3}} \tag{7}$$

The functions in the Eq. (7) are only differentiable for the variable of time. Thus, the Eq. (7) was transformed as:

$$K_{\mathrm{eq}} \left(c_{\mathrm{B(II),int}}{}^{3} \cdot \frac{\mathrm{d}c_{\mathrm{Ni^{2+}(III),int}}}{\mathrm{d}t} + 3 c_{\mathrm{Ni^{2+}(III),int}} \cdot c_{\mathrm{B(II),int}}{}^{2} \frac{\mathrm{d}c_{\mathrm{B(II),int}}}{\mathrm{d}t} \right) = c_{\mathrm{H^+(III),int}}{}^{2} \cdot \frac{\mathrm{d}c_{\mathrm{C(II),int}}}{\mathrm{d}t} \tag{8}$$

The diffusion of complex and carrier in the emulsion droplet ($0 \le r \le R_{\mathrm{f}}$):

$$(1-\varphi') \frac{\partial c_{\mathrm{B}}}{\partial t} = D_{\mathrm{B,eff}} \frac{1}{r^2} \frac{\partial}{\partial r} \left(r^2 \frac{\partial c_{\mathrm{B}}}{\partial t} \right) + 3 \frac{S'}{(V_{\mathrm{I}} + V_{\mathrm{II}})(1-\beta)^3} r_{\mathrm{s}} \tag{9}$$

$$(1-\varphi') \frac{\partial c_{\mathrm{C}}}{\partial t} = D_{\mathrm{C,eff}} \frac{1}{r^2} \frac{\partial}{\partial r} \left(r^2 \frac{\partial c_{\mathrm{C}}}{\partial t} \right) - \frac{S'}{(V_{\mathrm{I}} + V_{\mathrm{II}})(1-\beta)^3} r_{\mathrm{s}} \tag{10}$$

where the surface of S' is calculated by

$$S' = \frac{6}{d_\mu} V_{\mathrm{I}} \tag{11}$$

$$\varphi' = \varphi/(1-\beta)^3, \beta = 1 - R_{\mathrm{f}}/R, \quad \varphi = V_{\mathrm{I}}/(V_{\mathrm{I}} + V_{\mathrm{II}}) \tag{12}$$

The stripping reaction at the interface of II/I:

$$V_{\mathrm{I}} \frac{\mathrm{d}c_{\mathrm{Ni^{2+}(I)}}}{\mathrm{d}t} = S' \cdot r_{\mathrm{s}} \tag{13}$$

The initial concentration values of the nickel, the carrier, and the nickel–carrier complex at the external interface were assumed to be in equilibrium, and they were calculated by the Eqs. (7) and (18) using the algebraic equations-solving function of SOLVE in MATLB. Following are the initial conditions and the boundary conditions:

ICs:

$$\mathrm{for} t = 0, c_{\mathrm{Ni^{2+}(III)}} = c^0_{\mathrm{Ni^{2+}(III)}} \tag{14}$$

$$\text{for} t = 0, r = R_\mathrm{f}, \quad \left.\begin{aligned} c_{\mathrm{Ni^{2+}(III),int}} &= c^0_{\mathrm{Ni^{2+}(III),int}} \\ c_{\mathrm{C(II),int}} &= c^0_{\mathrm{C(II),int}} \\ c_{\mathrm{B(II),int}} &= c^0_{\mathrm{B(II),int}} \end{aligned}\right\} \tag{15}$$

$$\text{for} t = 0, 0 \le r < R_\mathrm{f}, \quad \left.\begin{aligned} c_{\mathrm{Ni^{2+}(I)}} &= 0 \\ c_\mathrm{C} &= 0 \\ c_\mathrm{B} &= c^0_\mathrm{B} \end{aligned}\right\} \tag{16}$$

BCs:

$$r = 0, \; D_\mathrm{C,eff}\frac{\partial c_\mathrm{C}}{\partial r} = 0, D_\mathrm{B,eff}\frac{\partial c_\mathrm{B}}{\partial r} = 0 \tag{17}$$

$$\begin{aligned} r &= R, \\ k_{Ni}\left(c_{Ni^{2+}(III)} - c_{Ni^{2+}(III),int}\right) &= k_C\left(c_C|_{r=R} - c_C|_{r=R_f}\right) \\ &= \tfrac{1}{3}k_B\left(c_B|_{r=R_f} - c_B|_{r=R}\right) \\ &= D_{C,eff}\tfrac{\partial c_C}{\partial r}\Big|_{r=R_f} \\ &= -\tfrac{1}{3}D_{B,eff}\tfrac{\partial c_B}{\partial r}\Big|_{r=R_f} \end{aligned} \tag{18}$$

A similar approach, like the Eq. (7), was used to transform the Eq. (18) as ordinary differential equations:

$$\frac{\mathrm{d}c_{\mathrm{Ni^{2+}(III)}}}{\mathrm{d}t} - \frac{\mathrm{d}c_{\mathrm{Ni^{2+}((III)),int}}}{\mathrm{d}t} = \frac{k_\mathrm{C}}{k_\mathrm{Ni}}\left(\frac{\mathrm{d}c_{\mathrm{C(II),int}}}{\mathrm{d}t} - \frac{\partial c_{\mathrm{C(II)}}}{\partial t}\bigg|_{r=R_f}\right) \tag{19}$$

$$\frac{\mathrm{d}c_{\mathrm{Ni^{2+}(III)}}}{\mathrm{d}t} - \frac{\mathrm{d}c_{\mathrm{Ni^{2+}(III),int}}}{\mathrm{d}t} = \frac{k_\mathrm{B}}{3k_\mathrm{Ni}}\left(\frac{\partial c_{\mathrm{B(II)}}}{\partial t}\bigg|_{r=R_f} - \frac{\mathrm{d}c_{\mathrm{B(II),int}}}{\mathrm{d}t}\right) \tag{20}$$

The above equations result in a system composed of nonlinear partial differential equations. We transformed the partial differential equations into the ordinary differential equations by the method of lines. In this method, the partial differential equations were discretized in space by the central differencing scheme. The numerical analysis result was listed in the Appendix A.

3. Estimation of parameters

The apparent stripping rate constant of k_s was estimated by optimization using the functions of FMINCON and LSQNONLIN in MATLAB. The mass transfer coefficient of nickel ions (k_Ni) was calculated according to the correlation [20]. The effective diffusivity ($D_\mathrm{B,eff}$ and $D_\mathrm{C,eff}$) and the mass transfer coefficient (k_B and k_C) of the carrier and the nickel–carrier complex were obtained in a similar way in a study proposed by Teramoto and Matsuyama [21]. The extraction equilibrium constant (K_eq) was obtained by experimentation. Wilke-Chang equation and Nernst equation were respectively used to calculate the diffusivity [22]. The values of the parameters under typical conditions are listed in Table 1.

Table 1
Values of the parameters for the extraction of nickel under the typical experimental condition

Parameters	Values
$D_\mathrm{B,eff}$	1.04×10^{-10} m^2/s
$D_\mathrm{C,eff}$	5.34×10^{-11} m^2/s
K_eq	6.90×10^{-9} m^3/mol
d_{32}	3.81×10^{-4} m
d_μ	3.10×10^{-7} m
δ	1.47×10^{-7} m
k_Ni	1.16×10^{-5} m/s
k_B	9.99×10^{-4} m/s
k_C	5.15×10^{-4} m/s

4. Experimental

4.1. Materials

The feed solution was prepared by dissolving $NiSO_4.6H_2O$ (Xilong Chemical Co., Ltd. (Shantou, China)) in distilled water and adding 0.1 mol/L NaAc–HAc solution (Fengchuan Chemical Reagent Co., Ltd. (Tianjin, China)). 0.5 M of sulfuric acid (Kaixin chemical Co., Ltd. (Hengyang, China)) was used as the internal stripping solution. The organic phase was composed of a paraffinic solvent (Damao Chemical Reagent Factory (Tianjin, China)), a surfactant of Span 80 (Kemiou Chemical Reagent Co., Ltd.(Tianjin, China)), a diluent of n-heptane (Hunan Huihong Reagent Co., Ltd. (Changsha, China)), and an extractant of PC 88A (Daihachi Chemical Industry (Osaka, Japan)).

4.2. Apparatus and procedure

In order to prepare the emulsion, the sulfuric acid solution was mixed with the organic phase by a homogenizer (Specimen and Model Factory (Shanghai, China)) at the speed of 8,500 rpm for 10 min. The volume ratio of $V_\mathrm{II}/V_\mathrm{I}$ was 3:1. The pH value of the feed solution was 4.7. Five percent (v/v) of Span 80 was used as surfactant. The ELM experiments were conducted in a glass reactor at low stirring speed. The emulsion was dispersed in the external feed solution (640 mL for most experiments). Samples were periodically taken and filtered during the extraction experiments. The emulsion was diluted 200 times using n-heptane, so that the diameter of the internal aqueous droplets can be determined by the laser particle analyzer (Mastersizer2000, Malvern Instruments Ltd. (Malvern, UK)).The photographic method was applied to measure the size of the emulsion drops by a Canon 60D camera (Canon (Tokyo, Japan)). The emulsion was broken by the electrostatic de-emulsification technique.

After using nitric acid (Kaixin chemical Co., Ltd.) for the pretreatment of digestion, the analysis of the nickel concentration was done with an atomic absorption spectrophotometer (AA6300C, Shimadzu, (Kyoto, Japan)). The pH value was determined by a pH meter (PHS-3D, Precision & Scientific Instrument CO., Ltd. (Shanghai, China)). Interfacial tension was obtained by the drop volume method. A viscometer (SNB-1, Precision & Scientific Instrument CO., Ltd.) was used to measure the viscosity of the membrane phase.

In order to obtain the equilibrium constant (K_{eq}), the extraction experiments were carried out in a closed vessel with magnetic stirring for 24 h at different values of pH, nickel concentration and PC 88A concentration. All extraction experiments were conducted in the volume ratio of O/A = 1:1 at the constant temperature of 20℃. The conditions of the ELM experiments were showed in Table 2. The degree of the agreement between the experimental data and the calculated results was represented by the average value of the squared residuals (σ^2), which was defined as:

$$\sigma^2 = \frac{\sum\left(\frac{c_{\mathrm{Ni}^{2+}(\mathrm{III}),\mathrm{calc}} - c_{\mathrm{Ni}^{2+}(\mathrm{III}),\mathrm{exp}}}{c^0_{\mathrm{Ni}^{2+}(\mathrm{III})}}\right)^2}{n} \tag{21}$$

5. Results and discussion

5.1. Effect of agitation speed

As represented in Fig. 2, the increase in the agitation speed resulted in a decrease in the emulsion droplet size, which in turn increased the interfacial area and the removal rate. Conversely, the co-transport of water also increased with the increase in the agitation speed. This led to the swelling of the emulsion droplets. With the increase in the stirring intensity, the breakage of the emulsion droplets intensified. Swelling and breakage are known to be harmful to the ELM process. As displayed in Fig. 2, the differences between the theoretical values and the experimental data gradually increased with the agitation speed.

5.2. Effect of the volume ratio

The volume ratio of the feed solution to the sulfuric acid solution indicates the treatment ratio of the ELM. Considering the cost of the reagent and the concentration ratio of the nickel ions, a high treatment ratio is desirous. However, when this parameter increased, even though the size of the emulsion droplets decreased, the specific interfacial area reduced, which resulted in the reduction of the extraction efficiency. Therefore, it will be conducive to obtain high removal efficiency by appropriately reducing the treatment ratio. As illustrated in Fig. 3, this model can satisfactorily predict the experimental results under these varying conditions of the treatment ratio.

5.3. Effect of the nickel ions initial concentration

The higher the initial concentration of nickel, the more extraction and stripping reagents required to achieve a high efficiency of the removal of nickel. When the nickel ions initial concentration increased, more nickel ions were removed using the same amount of agents in the ELM, while the ratio of the residual concentration to the initial concentration still increased. As a result, the removal rate decreases due

Table 2
The experimental conditions*

Parameters	Conditions	Typical conditions
Agitation speed	5.0, 5.8, and 6.7 s^{-1}	5.8 s^{-1}
Volume ratio of external phase to internal phase	16, 24, and 30	16
Initial concentration of nickel	500, 700, and 900 ppm	500 ppm
Initial concentration of carrier	4% (v/v), 5% (v/v), and 6% (v/v)	6% (v/v)

Note: *Other conditions: pH of feed solution: 4.7; $V_{\mathrm{II}}/V_{\mathrm{I}}$ = 3:1; span 80: 5% (v/v); sulfuric acid: 0.5 M.

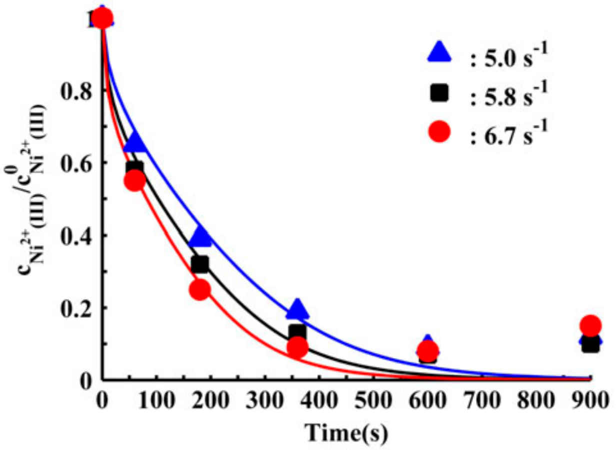

Fig. 2. Effect of agitation speed on the removal rate. (Operating conditions were: $V_{\mathrm{III}}/V_{\mathrm{I}} = 16$, $c^0_{\mathrm{Ni(III)}} = 500$ ppm, $c^0_{\mathrm{B}} = 6\%$ (v/v) (for other conditions see Table 2); the estimated values of k_{s} were: 1.6×10^{-9} m/s ($N = 5.0\ \mathrm{s}^{-1}$, $\sigma^2 = 0.013$), 1.7×10^{-9} m/s ($N = 5.8\ \mathrm{s}^{-1}$, $\sigma^2 = 0.012$), 1.9×10^{-9} m/s ($N = 6.7\ \mathrm{s}^{-1}$, $\sigma^2 = 0.015$); calculated results are represented using solid lines).

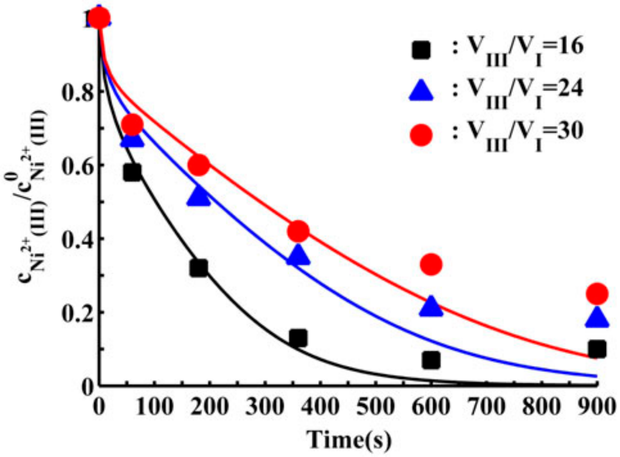

Fig. 3. Effect of the volume ratio on the removal rate. (Operating conditions were: $N = 5.8\ \mathrm{s}^{-1}$, $c^0_{\mathrm{Ni(III)}} = 500$ ppm, $c^0_{\mathrm{B}} = 6\%$ (v/v) (for other conditions see Table 2); The estimated values of k_{s} were: 1.7×10^{-9} m/s ($V_{\mathrm{III}}/V_{\mathrm{I}} = 16$, $\sigma^2 = 0.012$), 1.2×10^{-9} m/s ($V_{\mathrm{III}}/V_{\mathrm{I}} = 24$, $\sigma^2 = 0.022$), 1.3×10^{-9} m/s ($V_{\mathrm{III}}/V_{\mathrm{I}} = 30$, $\sigma^2 = 0.032$); calculated results are represented using solid lines).

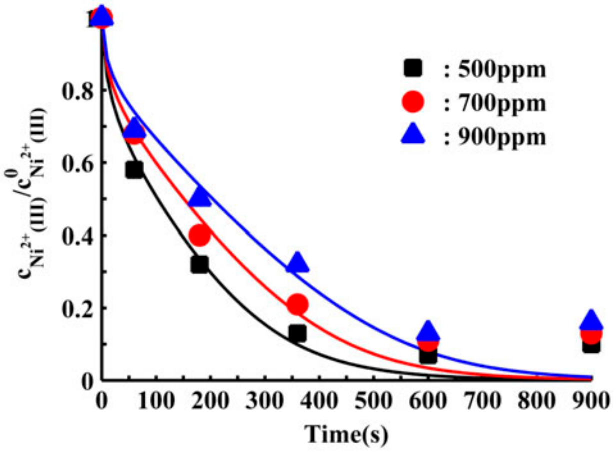

Fig. 4. Effect of the nickel ions initial concentration on the removal rate. (Operating conditions were: $N = 5.8\ \mathrm{s}^{-1}$, $V_{\mathrm{III}}/V_{\mathrm{I}} = 16$, $c^0_{\mathrm{B}} = 6\%$ (v/v) (for other conditions see Table 2); the estimated values of k_{s} were: 1.7×10^{-9} m/s ($c^0_{\mathrm{Ni(III)}} = 500$ ppm, $\sigma^2 = 0.012$), 1.6×10^{-9} m/s ($c^0_{\mathrm{Ni(III)}} = 700$ ppm, $\sigma^2 = 0.025$), 1.5×10^{-9} m/s ($c^0_{\mathrm{Ni(III)}} = 900$ ppm, $\sigma^2 = 0.028$); calculated results are represented using solid lines).

to a rise in the nickel ion concentration in the range of 500–900 ppm (see Fig. 4). It should be emphasized that unlike the traditional solvent extraction, the metal ions with low concentration can be adequately recovered through ELM. This is because the difference in the hydrogen ions concentration between the external aqueous solution and the internal sulfuric acid solution is the impetus for ELM.

5.4. Effect of the carrier concentration

As shown in Fig. 5, with the increase in the carrier concentration, the removal rate drastically increased.

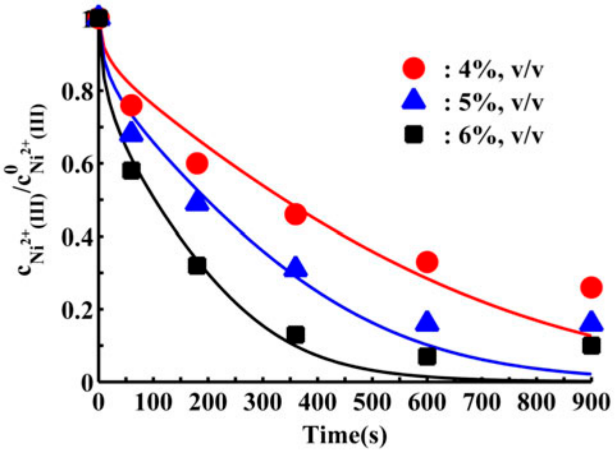

Fig. 5. Effect of the carrier concentration on the removal rate. (Operating conditions were: $N = 5.8\ \mathrm{s}^{-1}$, $V_{\mathrm{III}}/V_{\mathrm{I}} = 16$, $c^0_{\mathrm{Ni(III)}} = 500$ ppm (for other conditions see Table 2); the estimated values of k_{s} were: 1.7×10^{-9} m/s ($c^0_{\mathrm{B}} = 6\%$, v/v, $\sigma^2 = 0.012$), 1.6×10^{-9} m/s ($c^0_{\mathrm{B}} = 5\%$, v/v, $\sigma^2 = 0.021$), 1.5×10^{-9} m/s ($c^0_{\mathrm{B}} = 4\%$, v/v, $\sigma^2 = 0.026$); calculated results are represented using solid lines).

This is mainly due to the equilibrium of extraction reaction at the interface of III/II. This suggests that the extraction reaction is an important controlling step in this ELM process. However, the high concentration of the PC 88A increased the viscosity and the interfacial tension of the emulsion phase, which resulted in larger globules. The swelling of the emulsion worsened due to the increase in the carrier concentration. The amount of carrier used in the ELM process is relatively less than in the solvent extraction technology.

5.5. The calculated concentration at the external interface

For the purposes of intuitively describing the dynamic equilibrium of the concentration at the external interface, the variation in the concentration of substances at the external interface is shown in Fig. 6. At the beginning, the carrier concentration reduced rapidly due to the high extraction rate. With the increase in the diffusion rate within the emulsion globule and the stripping rate, the carrier concentration began to rebound. Meanwhile, the concentration of the nickel–carrier complex increased at first and then decreased. The variation trend in the concentration of the carrier and the complex at the external interface was similar to that in the emulsion globule. As shown in Fig. 6, the rapid increase in and the slight slow drop in the nickel concentration indicates that the mass transfer in the feed solution is not the rate-controlling step.

5.6. The calculated concentration distribution of carrier

Figs. 7 and 8 show the carrier concentration at all radii of the emulsion droplet decreased rapidly in the beginning, then increased gradually after reaching the lowest value, and finally approached its equilibrium value. The concentration gradient in the radial direction was high at the first, and then over time it decreased. The reduction in the carrier concentration in the early stage was mainly because the diffusion rate was very high. With the increase in the nickel–carrier complex concentration, the stripping reaction rate increased. The carrier concentration began to increase when the stripping reaction rate was higher than the diffusion rate.

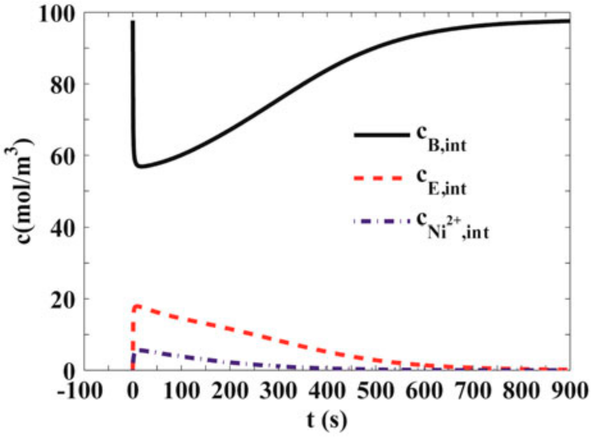

Fig. 6. Calculated concentration of the substances at the external interface for the different time on the typical conditions (see Table 2).

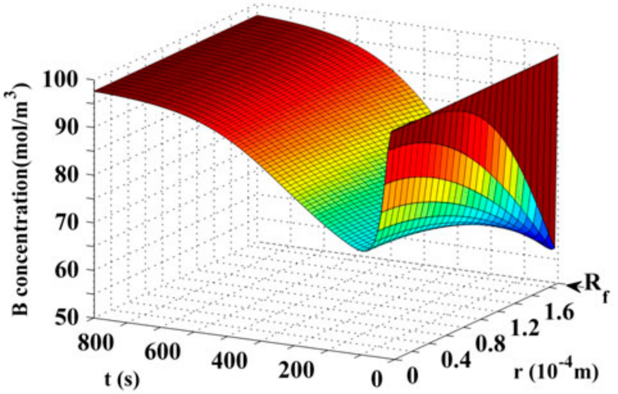

Fig. 7. Calculated concentration distribution of carrier in the emulsion droplet ($0 \le r \le R_f$) for the different time on the typical conditions (see Table 2).

5.7. The calculated concentration distribution of nickel–carrier complex

As shown, the nickel–carrier complex concentration at all radii of the emulsion droplet increased

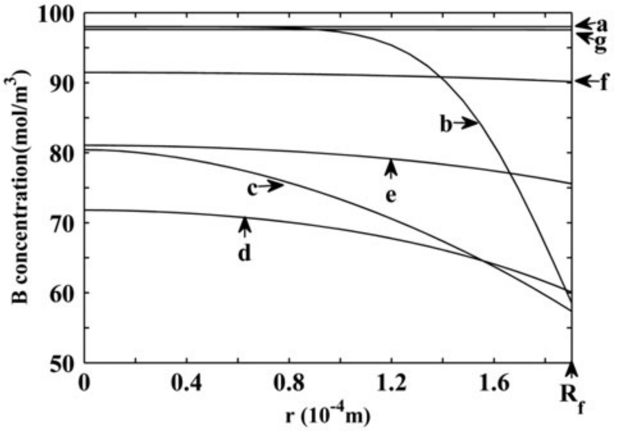

Fig. 8. Concentration profiles of carrier in the emulsion droplet ($0 \le r \le R_f$) on the typical conditions (see Table 2) for several certain time points (*s*) (a: 0, b: 5, c: 40, d: 100, e: 300, f: 500, and g: 900).

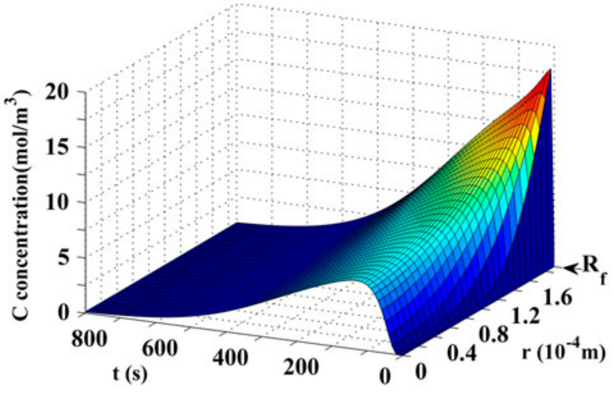

Fig. 9. Calculated concentration distribution of nickel–carrier complex in the emulsion droplet ($0 \le r \le R_f$) for the different time on the typical conditions (see Table 2).

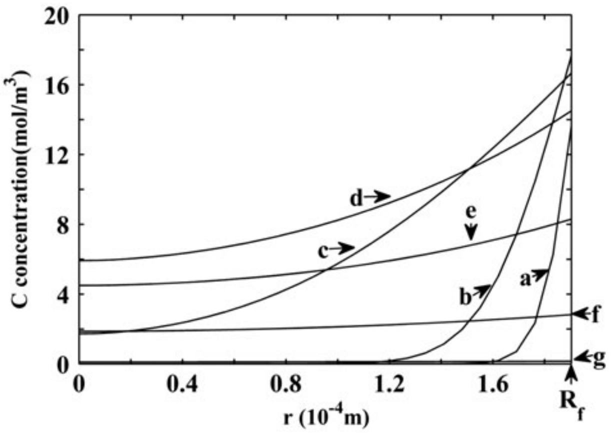

Fig. 10. Concentration profiles of nickel–carrier complex in the emulsion droplet ($0 \le r \le R_f$) on the typical conditions (see Table 2) for several certain time points (*s*) (a: 1, b: 5, c: 40, d: 100, e: 300, f: 500, and g: 900).

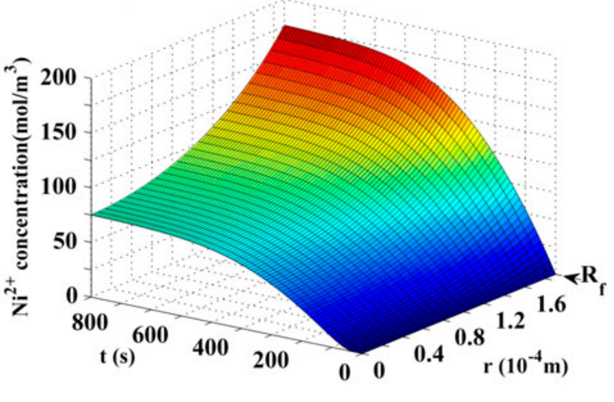

Fig. 11. Calculated concentration distribution of nickel in the emulsion droplet ($0 \le r \le R_f$) for the different time on the typical conditions (see Table 2).

quickly at the initial stage, then reduced slowly after reaching the peak value. The low concentration gradient in the later stage was mainly due to the fast mass transfer rate of the complex. It can be easy to speculate from Fig. 7–10 that when the nickel ions concentration was high in the beginning, the carrier concentration decreased quickly and the complex concentration increased rapidly. But on the contrary, at the end of the extraction process, the carrier concentration gradually rose again and the complex concentration slowly reduced to zero. Throughout the entire process, the carrier of PC 88A acted as a transporter in the reversible process.

5.8. The calculated the concentration distribution of nickel

The nickel concentration in the internal sulfuric acid solution increased with the increase in the extraction time at all radii of the emulsion droplet. The Figs. 11 and 12 also show that the nickel concentration in the emulsion droplet decreased away from the radius of R_f toward the center regardless of extraction time. As shown in Fig. 7–12, the calculated results for the concentration of the carrier, the complex, and the nickel in this model followed the law of mass conservation. For example, the concentration of carrier and complex in 15 min was approximately 97.6 and 0.1 mol/m^3, respectively. The above two concentration values were converted to the molarity of $(HR)_2$ (97.9 mol/m^3), which was approximately equal to the experimental value of the initial carrier concentration (98 mol/m^3).

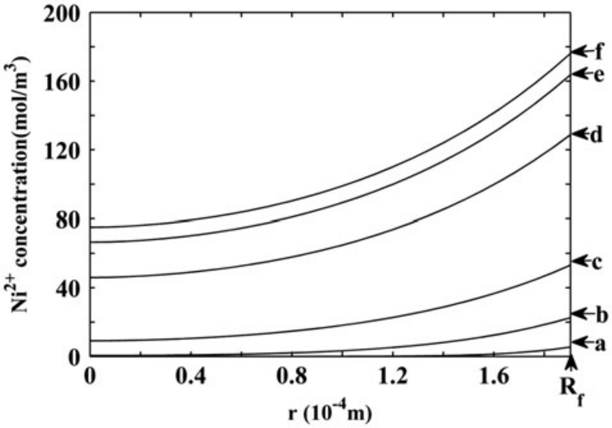

Fig. 12. Concentration profiles of nickel in the emulsion droplet ($0 \le r \le R_f$) on the typical conditions (see Table 2) for several certain time points (*s*) (a: 10, b: 40, c: 100, d: 300, e: 500, and f: 900).

6. Conclusions

The carrier of PC 88A had shown a satisfying removal ability of the nickel ions. Under typical conditions, the removal of nickel reached 93% in 10 min. A modified model was presented to describe the nickel extraction by the ELM. It was assumed that the concentrations at the external interface were in dynamic equilibrium. The mass transfer rate of the nickel ions in the external feed solution and that of the complexes at the interface of the emulsion droplet were assumed to be equal. Various experimental data for the different conditions on the removal rate of nickel by the ELM were numerically simulated. The experimental results showed that the extraction rate increased with the increase in the agitation speed and the PC 88A concentration. However, the extraction rate decreased with the increase in the initial nickel concentration and the volume ratio of V_{III}/V_I. The simulation results revealed that the total average value of the squared residuals between the experimental data and the calculated values was less than 0.022, which indicates that in spite of some approximations made in this model, the calculated results are in agreements with the experimental results. The concentration distribution figures show that the mass transfer rate in the emulsion droplet was high in the beginning and then decreased, whereas the stripping rate was low at first and then increased rapidly. The differences in the rate of the mass transfer and that of the stripping reaction became smaller with the delay in the extraction time and this resulted in the final equilibrium.

Acknowledgments

This research was supported by the Project of Hunan Provincial Natural Science Foundation of China (No. 14JJ5027), and the National Science and Technology Major Project of China on the Water Pollution Control and Treatment (No. 2010ZX07212-008).

Nomenclature

B — Carrier of PC 88A ($(HR)_2$)
c — Concentration (mol/m^3)
C — Nickel–carrier complex
d_μ — Internal aqueous drops diameter (Sauter mean diameter, m)
d_{32} — Emulsion drops diameter (Sauter mean diameter, m)
$D_{B,eff}$ — Carrier effective diffusivity (m^2/s)
$D_{C,eff}$ — Nickel–carrier complex effective diffusivity (m^2/s)
$(HR)_2$ — Dimer of PC 88A
k_B — Carrier mass transfer coefficient ($R_f \le r \le R$) (m/s)
k_C — Nickel–carrier complex mass transfer coefficient ($R_f \le r \le R$) (m/s)
k_{Ni} — Nickel ions mass transfer coefficient (m/s)
k_s — Stripping reaction rate constant (m/s)
K_{eq} — Extraction reaction equilibrium constant of nickel ions (mol/m^3)
N — Agitation speed (r/s)
$NiR_2.2(HR)_2$ — Nickel–carrier complex
r — Radial coordinate (m)
r_s — Stripping reaction rate per unit of the interface of II/I (mol/m^{2}s)
R — Emulsion droplets radius (m)
R_f — Radius of emulsion droplet inner core ($0 \le r \le R_f$) (m)
S — Total interfacial area between III/II (m^2)
S' — Total interfacial area between II/I (m^2)
t — Time (s)
V — Volume (m^3)

Greek letters

β — Parameter for the definition of φ'
δ — Thickness of thin oil layer (m)
σ^2 — Average value of the squared residuals (estimated value of the variance)
φ — Volume ratio of internal acid solution to emulsion phase
φ' — $\varphi/(1-\beta)^3$

Subscripts

B — Carrier ($(HR)_2$)
calc — Calculated value
C — Nickel–carrier complex
exp — Experimental value
$(HR)_2$ — Dimer of PC 88A
int — Interface
$NiR_2 \cdot 2(HR)_2$ — Nickel–carrier complex
I — Internal phase (sulfuric acid solution)
II — Membrane phase
III — External phase (feed solution)

Superscript

0 — Initial value

References

[1] P.V.R. Bhaskara Sarma, B.R. Reddy, Liquid-liquid extraction of nickel at macro-level concentration from sulphate/chloride solutions using phosphoric acid based extractants, Miner. Eng. 15 (2002) 461–464.

[2] R.K. Goyal, N.S. Jayakumar, M.A. Hashim, A comparative study of experimental optimization and response surface optimization of Cr removal by

emulsion ionic liquid membrane, J. Hazard. Mater. 195 (2011) 383–390.

[3] W. Lu, Y. Lu, F. Liu, K. Shang, W. Wang, Y. Yang, Extraction of gold (III) from hydrochloric acid solutions by CTAB/n-heptane/iso-amyl alcohol/Na_2SO_3 microemulsion, J. Hazard. Mater. 186 (2011) 2166–2170.

[4] J. Berrios, D.L. Pyle, G. Aroca, Gibberellic acid extraction from aqueous solutions and fermentation broths by using emulsion liquid membranes, J. Membr. Sci. 348 (2010) 91–98.

[5] B. Chanukya, N.K. Rastogi, Extraction of alcohol from wine and color extracts using liquid emulsion membrane, Sep. Purif. Technol. 105 (2013) 41–47.

[6] N. Othman, S.N. Zailani, N. Mili, Recovery of synthetic dye from simulated wastewater using emulsion liquid membrane process containing tri-dodecyl amine as a mobile carrier, J. Hazard. Mater. 198 (2011) 103–112.

[7] A.L. Ahmad, A. Kusumastuti, C.J.C. Derek, B.S. Ooi, Emulsion liquid membrane for heavy metal removal: An overview on emulsion stabilization and destabilization, Chem. Eng. J. 171 (2011) 870–882.

[8] R.A. Kumbasar, S. Kasap, Selective separation of nickel from cobalt in ammoniacal solutions by emulsion type liquid membranes using 8-hydroxyquinoline (8-HQ) as mobile carrier, Hydrometallurgy 95 (2009) 121–126.

[9] R.A. Kumbasar, Selective extraction of nickel from ammoniacal solutions containing nickel and cobalt by emulsion liquid membrane using 5,7-dibromo-8-hydroxyquinoline (DBHQ) as extractant, Miner. Eng. 22 (2009) 530–536.

[10] M. Chakraborty, C. Bhattacharya, S. Datta, Effect of drop size distribution on mass transfer analysis of the extraction of nickel (II) by emulsion liquid membrane, Colloids Surf. A 224 (2003) 65–74.

[11] P.S. Kulkarni, K.K. Tiwari, V.V. Mahajani, Membrane stability and enrichment of nickel in the liquid emulsion membrane process, J. Chem. Technol. Biotechnol. 75 (2000) 553–560.

[12] P. Kulkarni, K. Tiwari, V. Mahajani, Recovery of nickel via liquid emulsion membrane process using methane sulfonic acid as a strippant, Sep. Sci. Technol. 36 (2001) 639–656.

[13] A. Kopp, R. Marr, F. Moser, A new concept for mass transfer in liquid surfactant membranes without carriers and with carriers that pump, Inst. Chem. Eng. Symp. Ser. 54 (1978) 279–290.

[14] W. Ho, T. Hatton, E. Lightfoot, N. Li, Batch extraction with liquid surfactant membranes: A diffusion controlled model, AlChE J. 28 (1982) 662–670.

[15] N. Yan, A mass transfer model for type-II-facilitated transport in liquid membranes, Chem. Eng. Sci. 48 (1993) 3835–3843.

[16] P.F.M.M. Correia, J.M.R. de Carvalho, A comparison of models for 2-chlorophenol recovery from aqueous solutions by emulsion liquid membranes, Chem. Eng. Sci. 56 (2001) 5317–5325.

[17] M.T.A. Reis, J.M.R. Carvalho, Modelling of zinc extraction from sulphate solutions with bis(2-ethylhexyl)thiophosphoric acid by emulsion liquid membranes, J. Membr. Sci. 237 (2004) 97–107.

[18] M.T.A. Reis, O.M. de Freitas, L.M. Ferreira, J.M. Carvalho, Extraction of 2-(4-hydroxyphenyl) ethanol from aqueous solution by emulsion liquid membranes, J. Membr. Sci. 269 (2006) 161–170.

[19] M.T.A. Reis, O.M. de Freitas, L.M. Ferreira, J.M. Carvalho, Extraction of 4-hydroxycinnamic acid from aqueous solution by emulsion liquid membranes, Sep. Sci. Technol. 41 (2006) 841–860.

[20] S.C. Lee, J.H. Chang, B.S. Ahn, W.K. Lee, Mathematical modeling of penicillin G extraction in an emulsion liquid membrane system containing only a surfactant in the membrane phase, J. Membr. Sci. 149 (1998) 39–49.

[21] M. Teramoto, H. Matsuyama, Effect of facilitated diffusion in internal aqueous droplets on effective diffusivity and extraction rate of phenol in emulsion liquid membranes, J. Chem. Eng. Jpn. 19 (1986) 469–472.

[22] B.E. Poling, J.M. Prausnitz, O.C. John Paul, R.C. Reid, The properties of gases and liquids, fifth ed., McGraw-Hill, New York, NY, 2001, pp. 635–690.

Appendix A

In order to simplify the numerical solving process, the variable of radius (R_f) was separated as n intervals, as shown in Fig. 1. Thus, the Eqs. (9) and (10) and the Eq. (13) were transformed into a simple ordinary differential equation system as follow:

For the Eqs. (9)–(10):

$$(1-\varphi')\frac{\partial c_{\mathrm{B(i)}}}{\partial t} = D_{\mathrm{B,eff}}\left(\frac{c_{\mathrm{B(i+1)}} - c_{\mathrm{B(i-1)}}}{i\Delta r^2} + \frac{c_{\mathrm{B(i+1)}} - 2c_{\mathrm{B(i)}} + c_{\mathrm{B(i-1)}}}{\Delta r^2}\right) + 3\frac{S'}{(V_{\mathrm{I}} + V_{\mathrm{II}})(1-\beta)^3}k_{\mathrm{s}}c_{\mathrm{C}(i)} \tag{A.1}$$

$$(1-\varphi')\frac{\partial c_{\mathrm{C(i)}}}{\partial t} = D_{\mathrm{C,eff}}\left(\frac{c_{\mathrm{C(i+1)}} - c_{\mathrm{C(i-1)}}}{i\,\Delta r^2} + \frac{c_{\mathrm{C(i+1)}} - 2c_{\mathrm{C(i)}} + c_{\mathrm{C(i-1)}}}{\Delta r^2}\right) - \frac{S'}{(V_{\mathrm{I}} + V_{\mathrm{II}})(1-\beta)^3}k_{\mathrm{s}}c_{\mathrm{C}(i)} \tag{A.2}$$

where $i = 1, 2, 3, \ldots, n-1$, $R_{\mathrm{f}} = n\Delta r$

For $r = 0, i = 0$,

$$(1-\varphi')\frac{\partial c_{\mathrm{B(0)}}}{\partial t} = D_{\mathrm{B,eff}}\left(3\frac{2c_{B(1)} - 2c_{B(0)}}{\Delta r^2}\right) + 3\frac{S'}{(V_{\mathrm{I}} + V_{\mathrm{II}})(1-\beta)^3}k_{\mathrm{s}}c_{\mathrm{C(0)}} \tag{A.3}$$

$$(1-\varphi')\frac{\partial c_{\mathrm{C(0)}}}{\partial t} = D_{\mathrm{C,eff}}\left(3\frac{2c_{\mathrm{C(1)}} - 2c_{\mathrm{C(0)}}}{\Delta r^2}\right) - \frac{S'}{(V_{\mathrm{I}} + V_{\mathrm{II}})(1-\beta)^3}k_{\mathrm{s}}c_{\mathrm{C(0)}} \tag{A.4}$$

For $r = R_{\mathrm{f}}, i = n$,

$$\frac{\partial c_{\mathrm{B(n)}}}{\partial t} = \frac{D_{\mathrm{B,eff}}}{\Delta r^2(1-\varphi\prime)}\left((1+\frac{1}{n})(\frac{2k_{\mathrm{B}}\Delta r}{-D_{\mathrm{B,eff}}}(c_{\mathrm{B}(n)} - c_{\mathrm{B(II),int}})) + 2c_{\mathrm{B(n-1)}} - 2c_{\mathrm{B(n)}}\right) + 3\frac{S\prime}{(V_{\mathrm{I}} + V_{\mathrm{II}})(1-\beta)^3}k_{\mathrm{s}}c_{\mathrm{C(n)}} \tag{A.5}$$

$$\frac{\partial c_{\mathrm{C(n)}}}{\partial t} = \frac{D_{\mathrm{C,eff}}}{\Delta r^2(1-\varphi\prime)}\left(\left(1+\frac{1}{n}\right)\left(\frac{2k_{\mathrm{C}}\,\Delta r}{D_{\mathrm{C,eff}}}(c_{\mathrm{C(II),int}} - c_{\mathrm{C(n)}})\right) + 2c_{\mathrm{C(n-1)}} - 2c_{\mathrm{C(n)}}\right) - \frac{S'}{(V_{\mathrm{I}} + V_{\mathrm{II}})(1-\beta)^3}k_{\mathrm{s}}c_{\mathrm{C(n)}} \tag{A.6}$$

For the Eq. (13):

$$V_I\frac{dc_{Ni^{2+}(i)}}{dt} = S'k_{s}c_{\mathrm{C}(i)} \tag{A.7}$$

where $i = 0, 1, 2, 3, \ldots, n$.

As shown in the Eqs. (A.1)–(7), the Eq. (8), the Eqs. (19) and (20), and the Eq. (5), the partial differential equations with the initial and the boundary conditions were transformed into $3(n+1)+1$ ordinary differential equations with $3(n+1)+1$ unknowns, which was solved by calling an internal function called ODE23S in the MATLAB based on the Runge–Kutta method.